Preclinical evaluation of drug combinations identifies co-inhibition of Bcl-2/XL/W and MDM2 as a potential therapy in uveal melanoma

Decaudin, D.; Leitz, E.F.D.; Nemati, F.; Tarin, M.; Naguez, A.; Zerara, M.; ... ; Alsafadi, S.

European Journal of Cancer 126 (2020) 93–103

Available online at www.sciencedirect.com

ScienceDirect

journal homepage: www.ejcancer.com

Original Research

Preclinical evaluation of drug combinations identifies co-inhibition of Bcl-2/XL/W and MDM2 as a potential therapy in uveal melanoma

Didier Decaudin [a,b,1], Estelle Frisch Dit Leitz [c,1], Fariba Nemati [a,1], Malcy Tarin [c], Adnan Naguez [a], Mohamed Zerara [a], Benjamin Marande [c], Raquel Vivet-Noguer [c], Ensar Halilovic [d], Claire Fabre [d], Aart Jochemsen [e], Sergio Roman-Roman [c], Samar Alsafadi [c,*]

[a] *Laboratory of Preclinical Investigation, Department of Translational Research, Institut Curie, PSL University, Paris, France*
[b] *Department of Medical Oncology, Institut Curie, Paris, France*
[c] *Uveal Melanoma Translational Group, Department of Translational Research, Institut Curie, PSL Research University, Paris, France*
[d] *Novartis Institutes for Biomedical Research, Cambridge, MA, USA*
[e] *Department of Cell and Chemical Biology, Leiden University Medical Center, Leiden, the Netherlands*

Received 29 November 2019; accepted 6 December 2019
Available online 9 January 2020

KEYWORDS
Uveal melanoma;
Bcl-2/XL/W;
MDM2;
Drug synergism;
Drug screening;
Patient-derived xenografts

Abstract ***Introduction:*** Uveal melanoma (UM) is a rare and malignant intraocular tumour with a dismal prognosis. Despite a good control of the primary tumour by radiation or surgery, up to 50% of patients subsequently develop metastasis for which no efficient treatment is yet available.

Methodology: To identify therapeutic opportunities, we performed an *in vitro* screen of 30 combinations of different inhibitors of pathways that are dysregulated in UM. Effects of drug combinations on viability, cell cycle and apoptosis were assessed in eight UM cell lines. The best synergistic combinations were further evaluated in six UM patient-derived xenografts (PDXs).

Results: We demonstrated that the Bcl-2/X_L/W inhibitor (ABT263) sensitised the UM cell lines to other inhibitors, mainly to mammalian target of rapamycin (mTOR), mitogen-activated protein kinase kinase (MEK) and murine double minute 2 (MDM2) inhibitors. mTOR (RAD001) and MEK1/2 (trametinib) inhibitors were efficient as single agents, but their combinations with ABT263 displayed no synergism in UM PDXs. In contrast, the combination of

* *Corresponding author*:
E-mail address: samar.alsafadi@curie.fr, samaralsafadi@yahoo.com (S. Alsafadi).
[1] Joint first co-author.

https://doi.org/10.1016/j.ejca.2019.12.012

ABT263 with MDM2 inhibitor (HDM201) showed a trend for a synergistic effect.
Conclusion: We showed that inhibition of Bcl-2/X_L/W sensitised the UM cell lines to other treatments encouraging investigation of the underlying mechanisms. Furthermore, our findings highlighted Bcl-2/X_L/W and MDM2 co-inhibition as a promising strategy in UM.

1. Introduction

Uveal melanoma (UM) is a rare tumour deriving from melanocytes in the uveal tract. Considered to be the most common primary malignant intraocular tumour in adults, UM affects five individuals per million per year [1]. Despite a good control of the localised tumour by radiotherapy or surgery, up to 50% of UM patients develop metastases mainly in the liver. Once the disease has spread, the prognosis is poor with median survival of 9 months, and the treatment is challenging with absence of efficient therapeutic strategies [2,3].

In contrast to cutaneous melanoma, UM has a low mutational burden with two events per tumour beside few genomic alterations (losses of chromosome 1p, 3, 6q and 8p and gain of 8q) [4]. The first and most recurrent event in UM is the activation of Gαq signalling induced by mutations of *GNAQ/11* [5]. These mutations lead to activation in downstream effectors including protein kinase C (PKC), mitogen-activated protein kinases (MAPK) and yes-associated protein (YAP), implying a strong rational for therapeutic targeting of the related pathways in UM [6–9]. The second event consists of mutually exclusive mutations in the *BAP1*, *SF3B1 and EIF1AX* genes involved in processes of chromatin remodelling, splicing and translation, respectively.

Previous studies have shown that UM cell lines and patient-derived xenografts (PDXs) are susceptible to inhibition of single pathways such as PKC or mitogen-activated protein kinase kinase (MEK) [8,10,11]. However, clinical trials relying on monotherapeutic strategies have not resulted in any significant benefit in terms of overall survival of UM patients [12–14]. Such findings emphasised the need for combined strategies to improve clinical outcomes. We and others have previously shown that co-inhibition of targets such as PKC and murine double minute 2 (MDM2)/MDM4 or mammalian target of rapamycin (mTOR), and phosphoinositide 3-kinase (PI3K) synergistically improved the response in preclinical models [15–21].

Here, to identify further therapeutic opportunities in UM, we performed an *in vitro* screen of 30 combinations of different inhibitors of pathways dysregulated in UM. Cell viabilities under treatment with single or combined agents in eight UM cell lines were considered to calculate the synergy score for each drug combination. The eight best-ranked combinations were further evaluated for apoptosis, cell cycle profiles and related pathway engagement. Our data showed that the Bcl-2/X_L/W inhibitor (ABT263) displayed a highly synergistic potential in UM cell lines, mainly with mTOR, MEK and MDM2 inhibitors. These ABT263-based combinations were selected for assessment in six UM PDXs. mTOR (RAD001) and MEK (trametinib) inhibitors showed good efficacy in UM PDXs as single agents, but their combinations with ABT263 showed no clear benefit. In contrast, the combination of ABT263 with MDM2 inhibitor (HDM201) showed a trend for a synergistic effect encouraging further investigation of Bcl-2/X_L/W and MDM2 co-inhibition.

2. Materials and methods

2.1. Cell culture

MP38, MP46, MP65, MM28 and MM66 were established in our laboratory [11]. OMM1, OMM2.3 and OMM2.5 were kindly provided by P.A. van der Velden (Leiden University Medical Center, The Netherlands). The main characteristics of the used cell lines are reported in Supplementary Table S1. The immortalised hTERT RPE1 cell line was purchased from the ATCC. Cells were cultured in RPMI-1640 supplemented with 10% foetal bovine serum (FBS) (OMM1, OMM2.3, OMM2.5, RPE1) or 20% FBS (MP38, MP46, MP65, MM28, MM66). All cells were maintained at 37°C in a humidified atmosphere with 5% CO2 and were tested and certified as mycoplasma free.

2.2. Compounds

All drugs and inhibitors (Supplementary Table S2) were purchased from SelleckChem except HDM201 generously provided by Novartis Institutes for Biomedical Research. For the *in vitro* study, all drugs were dissolved in dimethyl sulfoxide (DMSO) at 10 mM and stored at −20°C. For the *in vivo* study, drug preparations are detailed in the Supplementary Table S3.

2.3. Drug combination cell viability screen

Cells were plated in 96-well plates at appropriate concentration. Twenty-four hours later, drugs were added as single agents or in combinations. Serial 1:3 dilutions were prepared starting from the maximal concentration for each

drug (Supplementary Table S2), resulting in six different concentrations (Supplementary Fig. S1). Cell viability was assessed after 5 days of treatment using MTT (3-(4,5-dimethylthiazol-2-yl)-2,5-diphenyltetrazolium bromide) assay (Sigma). Three technical replicates and three independent biological replicates were performed for each treatment and for each cell model. As detailed in a previous paper, Bliss independence model was used to determine the combination synergistic potential [15].

2.4. Caspase-3/7 activity assay and cell cycle analysis

Cells were treated with combinations at synergistic doses defined according to the screening. A fluorescence-based assay was used to determine the activity of caspases-3 and caspase-7 (Apo-One Homogeneous Caspase-3/7 Assay, Promega). The assay was performed according to the manufacturer's recommendations.

For cell cycle profiling, cells were collected, washed twice with phosphate buffered saline (PBS) and fixed with cold ethanol. Afterwards, cells were pelleted and resuspended in PBS containing 50 µg/ml propidium iodide (Sigma Aldrich) and 2.5U/mL RNAse I (ThermoFisher). Samples were analysed using FACScalibur (Becton Dickinson) and CellQuest software (Becton Dickinson).

2.5. Immunoblot analyses

Protein extracts, separated by SDS-PAGE and transferred onto polyvinylidene difluoride (PVDF) membranes, were probed with antibodies against p21 (#2947), pS6 (#2215), S6 (#2317), poly ADP-ribose polymerase (PARP, #9542),

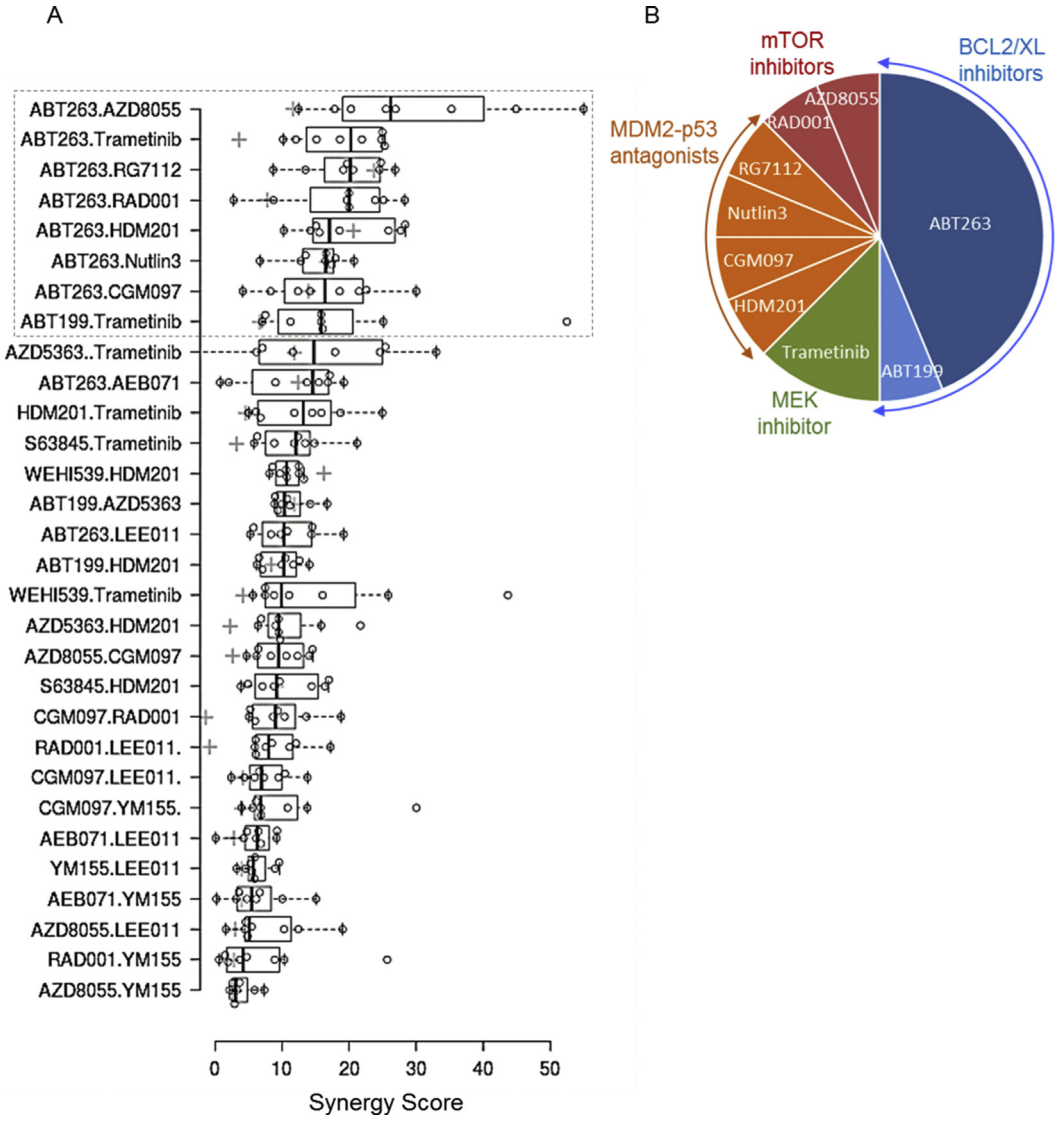

Fig. 1. **Ranking of drug combinations tested *in vitro* according to synergy scores**. (A) The screening of drug combinations was done in eight uveal melanoma cell lines and in RPE1 (retinal pigment epithelial cells). The best-ranked eight combinations in uveal melanoma cell lines are indicated. Each circle represents the synergy score in one cell line. The light grey plus (+) represents the synergy score in RPE1. (B) Representation of compound and targeted pathway enrichment in the best-ranked eight combinations.

pERK (#9101), extracellular signal-regulated kinase (ERK) (#9102) and actin (#3700), all purchased from Cell Signaling Technology (Beverly, MA). Immunolabelled proteins were detected using Odyssey secondary antibodies coupled to a 700 or 800 nm and the Odyssey Infrared Imaging System (Li-cor). Actin immunoblotting was used to quantify and normalise results.

2.6. Uveal melanoma PDX models and in vivo treatments

We used PDXs derived from liver metastatic tumour samples (MM26, MM66, MM224, MM252, MM267, MM300 and MM309), and one established from a cutaneous metastasis (MM33). The main molecular features of these models are presented in the Supplementary Table S4. The experimental protocol of the *in vivo* study is detailed in the supplementary methods [10,30].

3. Results

3.1. Identification of synergistic combinations in a panel of uveal melanoma cell lines

We performed a screen of 30 dual drug combinations in a panel of eight UM cell lines harbouring the most frequent genetic features of the metastatic disease with *GNAQ* or *GNA11* mutations associated or not with BAP1 deficiency. The assessed cell lines were derived either from metastases or from primary tumours lacking BAP1 expression, a feature correlated with poor prognosis (Supplementary Table S1). Immortalised RPE1 cell line was included as a control cell line with no mutations affecting the targeted pathways. The tested compounds were selected based on the current knowledge of pathways dysregulated in UM for which specific inhibitors are available (Supplementary Table S2). All combinations were assessed for synergy based on cell viability and according to the Bliss independence model. Fig. 1A shows the ranking of the tested combinations according to their median Best Excess Over Bliss values in UM cell lines.

The best-ranked eight combinations were enriched by Bcl-2/X_L/W inhibitor ABT263 (Fig. 1B). ABT263 exhibited low efficacy as a single agent but synergised with most tested compounds in UM cell lines. The synergistic effect decreased when replacing ABT263 by selective inhibitors of Bcl-2 (ABT199), Bcl-X_L (WEHI539) or MCL1 (S63845). This finding suggests that simultaneous inhibition of different BCL-2 family members is needed to promote the synergism. MDM2 inhibitors were the second best represented compounds in the top-ranked eight combinations. Thus, the results of our drug screening suggest that the Bcl-2/X_L/W inhibitor ABT263 sensitises the UM cells to inhibitors of several pathways including MDM2, mTOR and MEK inhibitors.

3.2. Assessment of apoptosis and cell cycle under treatment with the best synergistic drug combinations

Since the synergy was evaluated based on cell viability reduction rather than cell death induction, we investigated the effects of the best-ranked eight combinations on apoptosis induction and cell cycle in the OMM1 cells.

We evaluated apoptosis based on caspase 3/7 activity at 72 h of treatment. Fig. 2 shows that the Bcl-2/X_L/W and Bcl-2 inhibitors, ABT263 and ABT199, induced caspase 3/7 activation as single agents. The other tested single agents did not affect caspase 3/7 activation. Interestingly, the eight drug combinations displayed a considerable synergistic potential in terms of caspase 3/7 activation as compared with single agents implying an added value of combining these agents.

Additionally, we characterised the effect of the selected drug combinations on cell cycle. As shown in Supplementary Fig. S2, the sub-G1 profiles confirmed an increased induction of cell death under treatment with ABT263 and MDM2 inhibitors including CGM097, Nutlin3, HDM201 and RG112 (32–40% in combined treatments versus 21% in ABT263 and 8–10% in MDM2 inhibitors) along with a decrease in the proportion of proliferating cells in S phase. On the other hand, single-agent treatments did not induce any significant changes in cell cycle.

We further analysed the expression of proteins engaged in the related pathways in treated OMM1 cells. As shown in Fig. 3A and B, we observed increased levels of PARP

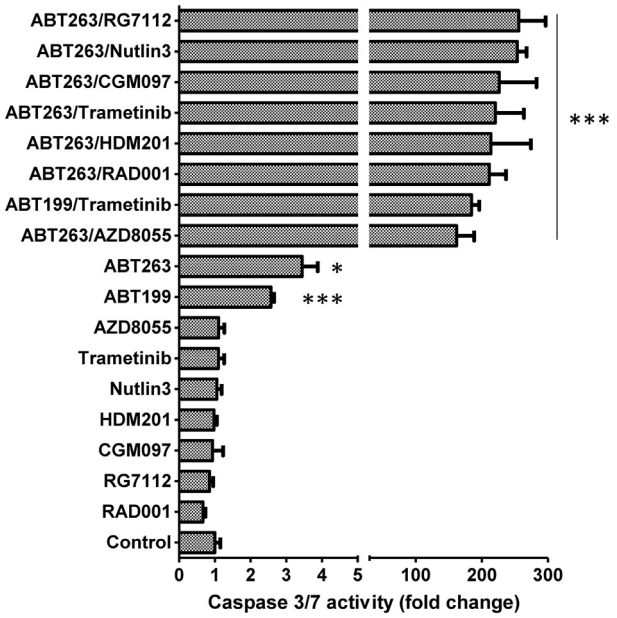

Fig. 2. **Apoptosis induction in OMM1 cells treated with eight best-ranked combinations**. Quantification of apoptosis induction after treatment with the eight best-ranked combinations. A fluorescence-based assay was used to determine the activity of caspase-3 and caspase-7, indicators of apoptosis induction.

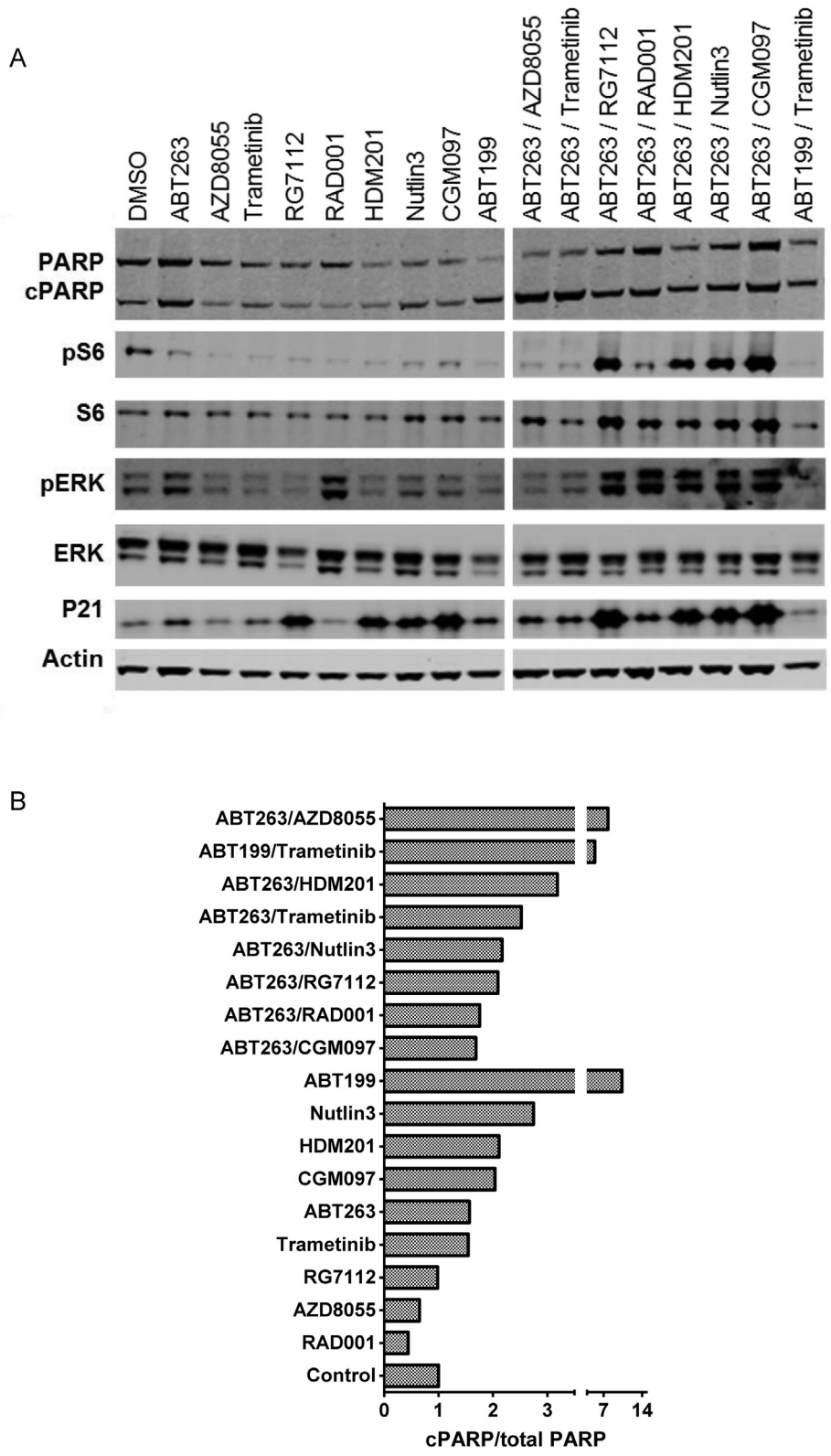

Fig. 3. **Immunoblot analysis for cleaved PARP and key signalling pathways in uveal melanoma**. (A) Western blots of OMM1 cells treated with the best-ranked drug combinations for 5 days. Cell lysates were analysed with the indicated antibodies. (B) Ratio of PARP cleavage product to total PARP as evaluated by Western blot intensities.

cleavage under combined treatments with ABT263 and HDM201/trametinib/AZD8055 as compared with single treatments. p21 was mainly induced following treatment with different MDM2 inhibitors, consistent with the activation of p53 pathway (Fig. 3A). MEK/ERK pathway was inhibited in treatments targeting MEK and MDM2 (Fig. 3A). Intriguingly, we observed a negative feedback regulation of ERK phosphorylation and S6 expression under combinations of ABT263 and MDM2 inhibitors.

Overall, our results show that the Bcl-2/X_L/W inhibitor ABT263 displays a highly synergistic potential with several agents in UM cell lines. MDM2, mTOR and MEK inhibitors were then selected as potential candidates to be combined with ABT263 for a further *in vivo* evaluation.

3.3. In vivo evaluation of ABT263-based combinations in UM PDXs

Based on these *in vitro* findings, three ABT263-based combinations were further assessed in six UM PDXs. These models were all established from liver metastases except for MM33 that was obtained from a cutaneous metastasis. Supplementary Table S4 recapitulates the histology and *GNAQ/GNA11*, *BAP1* and *SF3B1* statuses of these models. The list of tested drugs, doses and the schedule of administration are provided in Supplementary Table S3. We tested the Bcl-2/X_L/W inhibitor ABT263, alone or combined with the MDM2 inhibitor HDM201, the mTOR inhibitor RAD001 and with the MEK1/2 inhibitor trametinib. For each model, three mice were treated per group. Two of the drugs were administered in two different schedules to evaluate their efficacy while minimising the toxic effects: HDM201 was administered twice a week, every week (HDM-1) or every two weeks (HDM-2), while RAD001 was administered 5 days per week (RAD-1) or twice a week, every week (RAD-2) or every 4 weeks (RAD-3).

Single-agent ABT263 did not induce significant tumour regression in the tested models (Figs. 4–6 and Supplementary Figs. S3–S5). In contrast, HDM201 alone induced a slight but not dose-dependent antitumour efficacy with an overall response rate (ORR) lower than −0.5 of 35% and 43% in the continuous and discontinuous schedules of administration, respectively (Fig. 4A). Interestingly, we observed a slight synergistic effect of the combination of ABT263 + HDM-1 (continuous schedule of administration), but not HDM-2 (discontinuous schedule), with an ORR lower than

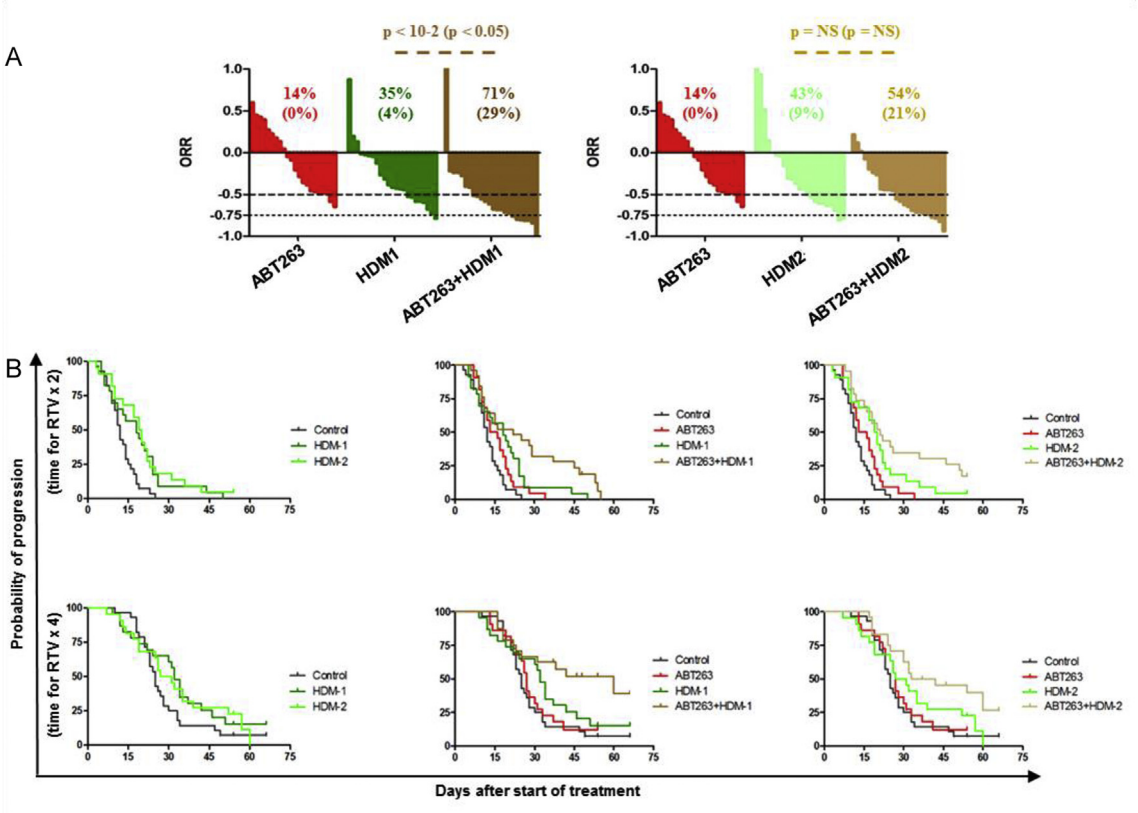

Fig. 4. ***In vivo* efficacy of ABT263 ± HDM201 in six uveal melanoma patient-derived xenografts**. (A) Overall response rate (ORR); the percentage in brackets correspond to an ORR lower than −0.75. (B) Probability of progression after each tested treatment; the methodology is detailed in the Materials & Methods section; the time to reach relative tumour volume (RTV) x 2 and RTV x 4 for each treated mouse has been calculated.

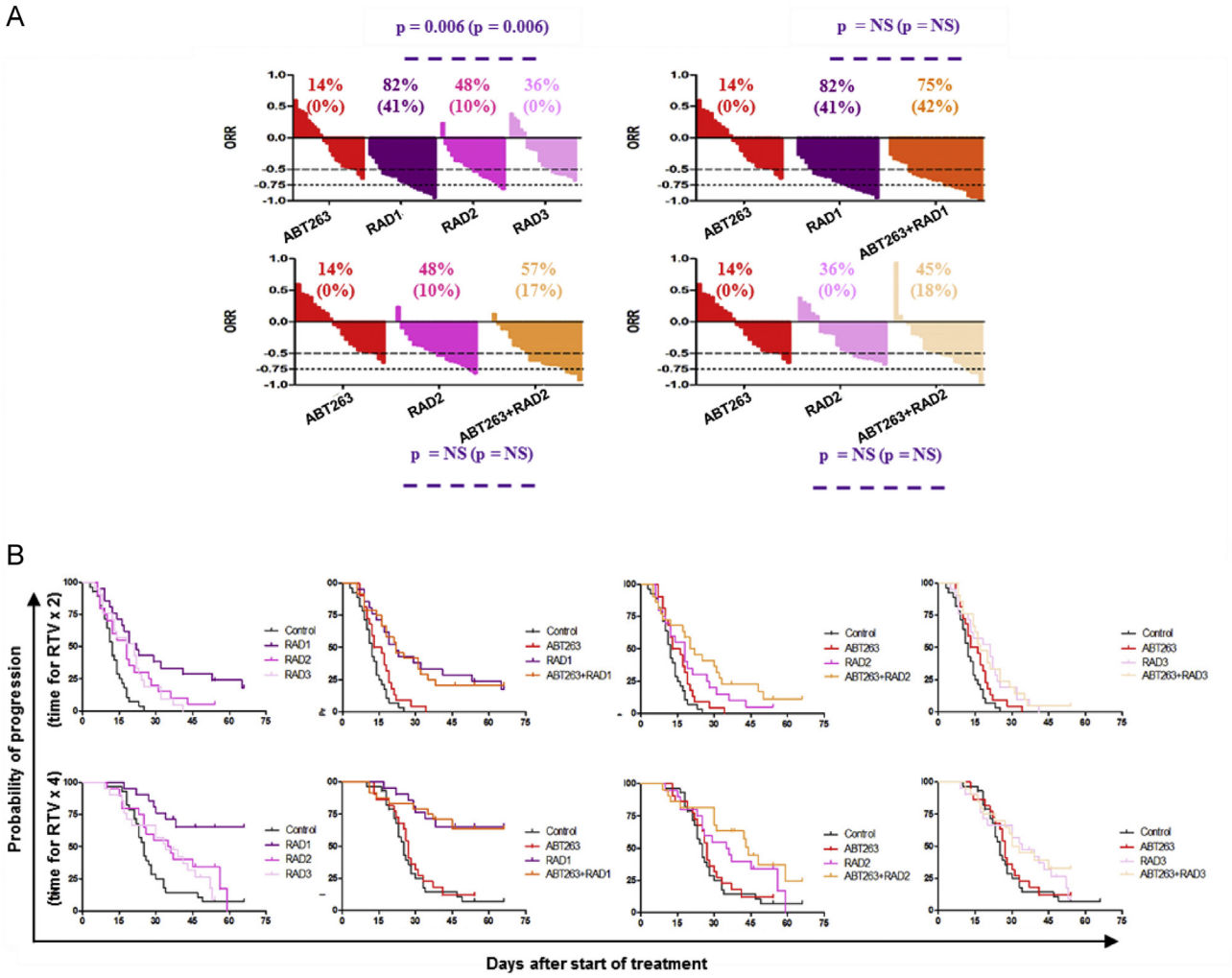

Fig. 5. ***In vivo*** **efficacy of ABT263 ± RAD001 in six uveal melanoma patient-derived xenografts**. (A) Overall response rate (ORR); the percentage in brackets correspond to an ORR lower than −0.75. (B) Probability of progression after each tested treatment; the methodology is detailed in the Materials & Methods section; the time to reach RTV x 2 and RTV x 4 for each treated mouse has been calculated.

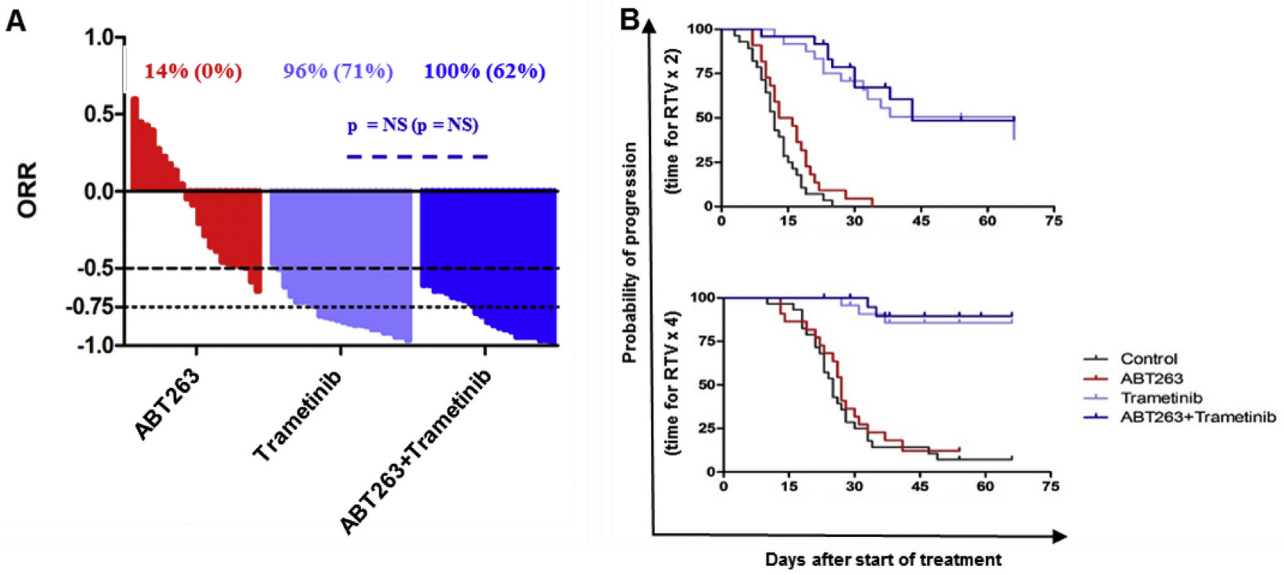

Fig. 6. ***In vivo*** **efficacy of ABT263 ± trametinib in six uveal melanoma patient-derived xenografts**. (A) Overall response rate (ORR); the percentage in brackets correspond to an ORR lower than −0.75. (B) Probability of progression after each tested treatment; the methodology is detailed in the Materials & Methods section; the time to reach RTV x 2 and RTV x 4 for each treated mouse has been calculated.

−0.5 of 35% and 71% after HDM-1 alone and ABT263 + HDM-1, respectively (Fig. 4A). Yet, we did not observe any significant impact on the probability of tumour progression (Fig. 4B). Individual curves are displayed in Supplementary Fig. S3.

Concerning the single-agent treatments, trametinib and full-dose RAD001 (RAD-1, 5 days/week) showed the best antitumour response. The antitumour effect of full-dose RAD001 was significantly higher ($p = 0.006$) than RAD001 administered with the other two schedules, showing a high dose-dependent antitumour efficacy (Fig. 5A). We did not observe any additive effect for ABT263 + RAD001, regardless of RAD001 administration schedule (Fig. 5B). Individual curves are displayed in Supplementary Fig. S4.

Despite a significant antitumour activity of trametinib alone with an ORR lower than −0.5 of 96% (Fig. 6A), its combination with ABT263 did not show any additive effect (Fig. 6B). Individual curves are displayed in Supplementary Fig. S5.

Analysis of protein expression of residual tumours in treated MM300 PDXs confirmed S6 or ERK dephosphorylation by RAD001 and trametinib (Fig. 7A and B). ABT263 + HDM-1 (continuous schedule of administration), but not HDM-2 (discontinuous schedule), showed significant increase of p21, indicator of p53 activation. Intriguingly, no significant PARP cleavage was detected. The absence of this indicator of apoptosis can be explained by the heterogeneity of cell exposure to treatments *in vivo* or by the fact that residual tumours represent cells resisting upon treatment.

We then investigated whether ABT199, a highly selective inhibitor of Bcl-2 with limited clinical toxicity, is as efficacious as ABT263 in combination with HDM201

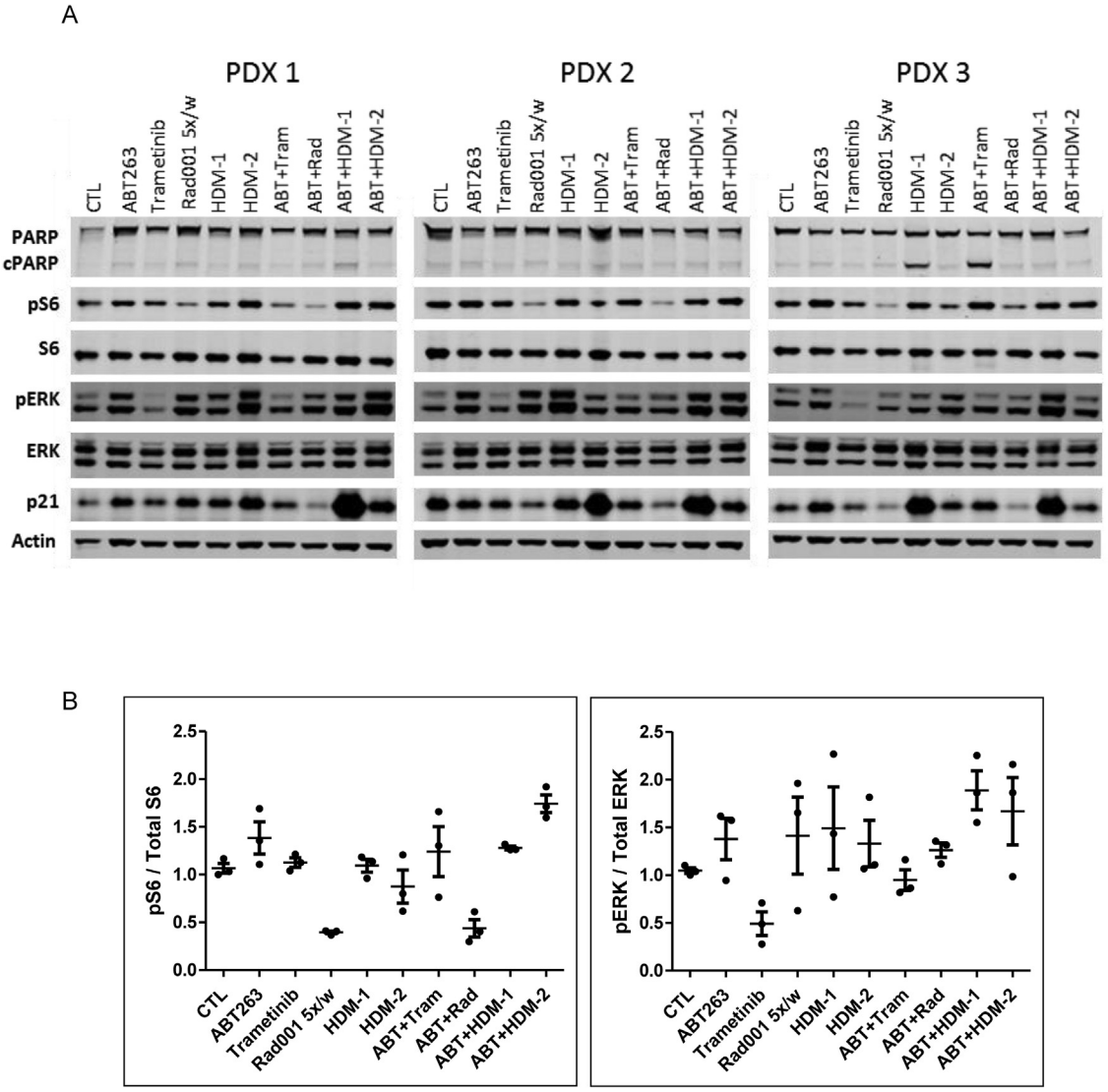

Fig. 7. **Protein expression levels after combination treatment *in vivo***. (A) Immunoblot analysis of key signalling pathways in three different mice of MM300 PDX model after treatment with ABT263 combined with HDM201, RAD001 or trametinib. (B) Ratios of blot intensities of pS6 to total S6 and pERK to total ERK as determined by ImageJ. ERK, extracellular signal-regulated kinase.

under the continuous schedule of treatment in two UM PDX models. In contrast to ABT263, ABT199 did not provide any significant increase of HDM201 antitumour effect (Supplementary Fig. S6).

Thus, based on our *in vivo* findings, trametinib and RAD001 showed good efficacy as single agents, but their tested combinations provided no significant antitumor benefit. Interestingly, the combination of ABT263 with HDM201 showed a trend of synergistic effect that was not observed when replacing ABT263 by the Bcl-2 selective inhibitor ABT199.

4. Discussion

UM is a rare tumour of which metastatic lesions remain a main therapeutic challenge in the absence of efficient treatments. The identification of the UM major driver events has oriented the preclinical and clinical trials towards inhibitors of the pathways dysregulated by these events. Nevertheless, single pathway inhibition has not improved patient outcomes so far, arguing for the need of combinatorial approaches.

Our screening of 30 combinations in eight UM cell lines identified the Bcl-2/X_L/W inhibitor ABT263 as the molecule with the highest synergistic potential followed by the MDM2 (RG7112, HDM201, Nutlin3, CGM097) and mTOR (AZD8055, RAD001) inhibitors. Our findings demonstrated that apoptosis was increased following treatment with these combinations as compared with single-agent treatments. The cell cycle profiles confirmed an increased induction of apoptosis in cells treated with ABT263 and MDM2 inhibitors along with a decrease in the proliferation rate. While single-agent ABT263 exhibited low efficacy in UM cell lines, it enhanced considerably the effect of the other compounds. These findings are consistent with previous studies reporting a high synergistic potential of Bcl-2/X_L/W inhibition when combined with cytotoxic agents in different types of cancer [22–27].

Based on the observed synergism between the Bcl-2/X_L/W inhibitor and MDM2, mTOR and MEK inhibitors (HDM201, RAD001 and trametinib, respectively), these combinations were further evaluated in metastatic UM PDXs. As in cell lines, single-agent ABT263 presented a modest effect on the tumour volume, while the other inhibitors (HDM201, RAD001 and trametinib) decreased considerably the tumour volume as monotherapies. The tested combinations did not show any synergistic effect in terms of progression probability except for the combination of ABT263 with HDM201. BCL2 and MDM2 are both reported to be highly expressed in UM arguing a further therapeutic interest of this co-inhibition [4,28,29]. Chapeau et al. conducted a large-scale transposon-based insertional mutagenesis screen to investigate the resistance to HDM201 in mice [26]. Among the most frequent alterations conferring resistance, they observed transposon-mediated gain-of-function alterations in Bcl-X_L and confirmed its overexpression in HDM201-resistant tumours. Furthermore, they demonstrated a significant synergy of MDM2 and Bcl-X_L co-inhibition in p53 wild-type cell lines [26]. Interestingly, our data are in line with these recent findings implying that synergism is due to Bcl-2/X_L/W inhibition rather than specific inhibition of Bcl-2 (ABT199), Bcl-X_L (WEHI539) or MCL1 (S63845).

5. Conclusion

Overall, our study highlights the potential of Bcl-2/X_L/W inhibition to enhance the activity of MDM2 inhibition in UM. Further characterisation of the underlying mechanisms to determine why and how such drug combinations synergise to induce apoptosis in UM cells would improve the current therapeutic strategies.

Conflicts of interest statement

E.H. and C.F. are employees at Novartis. The other authors declare no conflict of interest.

Acknowledgements

This study is supported by the European Union's Horizon 2020 research and innovation programme (UM Cure 2020 project, grant agreement no. 667787) and SIRIC Curie (Grant INCa-DGOS-Inserm_12554). The authors acknowledge Emilie Vinolo (seeding science SPRL, Limelette, Belgium) for her editorial support, as well as the other members of the UM Cure 2020 Consortium: Viviana Anelli, Marina Mione (Università degli Studi di Trento, Centre for Integrative Biology, Trento, Italy), Niels J. Brouwer, Rogier Nell, Pieter van der Velden, Annemijn Wierenga, Ellen Kapiteijn (Department of Medical Oncology, Leiden University Medical Center, Leiden, The Netherlands), Erica Cirri, Antoine Prestat, Jennifer Sengenes (PEP-Therapy SAS, Paris, France), Sophie Piperno-Neumann, Manuel Rodrigues (Department of Medical Oncology, Institut Curie, PSL Research University, Paris, France) Laurence Desjardins, Nathalie Cassoux (Department of Ocular Oncology, Institut Curie, PSL Research University, Paris, France), Raymond Barnhill (Department of Translational Research, Institut Curie, PSL Research University, Paris, France), Martyna Elas, Bozena Romanowska-Dixon (Jagiellonian University Medical College, Krakow, Poland), Martine J. Jager (Department of Ophtalmology, Leiden University Medical Center, Leiden, The Netherlands), Kseniya Glinkina (Department of Cell and Chemical Biology, Leiden

University Medical Center, Leiden, The Netherlands), Arwin Groenewoud, Ewa Snaar-Jagalska (Universiteit Leiden, Leiden, The Netherlands), Richard Marais, Pauline Hascoet, Valeria Pavet Rodrigues (Molecular Oncology Group, Cancer Research UK Manchester Institute, University of Manchester, Manchester, UK), Liesbeth Houkes, Dianne van den Heuvel (PamGene Internationa BV, BJ's-Hertogenbosch, The Netherlands), Sarah E. Coupland, Helen Kalirai, Matthew Traynor (Department of Molecular and Clinical Cancer Medicine, University of Liverpool, Liverpool, UK), Ana Lalanne, Olivier Lantz (INSERM U932 and Laboratory of Clinical Immunology, Institut Curie, PSL Research University, Paris, France), Pascale Mariani (Department of ophthalmologic surgery, Institut Curie, PSL Research University, Paris, France), Marc-Henri Stern, Lenha Mobuchon (Department of Genetics, Institut Curie, PSL Research University, Paris, France), André Valente, Guilherme Neri Pires, Constança Roquette (Champalimaud Foundation, Lisbon, Portugal), Bettina Ryll, Andrew Evans, Iain Galloway and Dick Plomp (Melanoma Patient Network Europe, Uppsala, Sweden).

The authors wish to thank the Animal Platform CRP2-UMS 3612 CNRS-US25 Inserm-IRD (Faculty of Pharmacy, Paris Descartes University, Paris), and the Animal Platform of Institut Curie. They also thank Justine Fleury and Steven Birot de la Pommeraye for their technical assistance (Laboratory of preclinical investigation, Institut Curie).

Appendix A. Supplementary data

Supplementary data to this article can be found online at https://doi.org/10.1016/j.ejca.2019.12.012.

References

[1] Mahendraraj K, Lau CSM, Lee I, Chamberlain RS. Trends in incidence, survival, and management of uveal melanoma: a population-based study of 7,516 patients from the surveillance, epidemiology, and end results database (1973–2012). Clin Ophthalmol 2016. https://doi.org/10.2147/OPTH.S113623.

[2] Singh M, Durairaj P, Yeung J. Uveal melanoma: a review of the literature. Oncol Ther 2018;6:87–104. https://doi.org/10.1007/s40487-018-0056-8.

[3] Vivet-Noguer R, Tarin M, Roman-Roman S, Alsafadi S. Emerging therapeutic opportunities based on current knowledge of uveal melanoma biology. Cancers 2019. https://doi.org/10.3390/cancers11071019.

[4] Helgadottir H, Höiom V. The genetics of uveal melanoma: current insights. Appl Clin Genet 2016. https://doi.org/10.2147/TACG.S69210.

[5] Van Raamsdonk CD, Griewank KG, Crosby MB, Garrido MC, Vemula S, Wiesner T, et al. Mutations in GNA11 in uveal melanoma. N Engl J Med 2010. https://doi.org/10.1056/nejmoa1000584.

[6] Feng X, Degese MS, Iglesias-Bartolome R, Vaque JP, Molinolo AA, Rodrigues M, et al. Hippo-independent activation of YAP by the GNAQ uveal melanoma oncogene through a trio-regulated rho GTPase signaling circuitry. Cancer Cell 2014. https://doi.org/10.1016/j.ccr.2014.04.016.

[7] Yu FX, Zhao B, Guan KL. Hippo pathway in organ size control, tissue homeostasis, and cancer. Cell 2015. https://doi.org/10.1016/j.cell.2015.10.044.

[8] Wu X, Zhu M, Fletcher JA, Giobbie-Hurder A, Hodi FS. The protein kinase C inhibitor enzastaurin exhibits antitumor activity against uveal melanoma. PLoS One 2012. https://doi.org/10.1371/journal.pone.0029622.

[9] Feng X, Arang N, Rigiracciolo DC, Lee JS, Yeerna H, Wang Z, et al. A Platform of synthetic lethal gene interaction networks reveals that the GNAQ uveal melanoma oncogene controls the hippo pathway through FAK. Cancer Cell 2019. https://doi.org/10.1016/j.ccell.2019.01.009.

[10] Decaudin D, Botty R El, Diallo B, Massonnet G, Fleury J, Naguez A, et al. Selumetinib-based therapy in uveal melanoma patient-derived xenografts. Oncotarget 2018. https://doi.org/10.18632/oncotarget.24670.

[11] Amirouchene-Angelozzi N, Nemati F, Gentien D, Nicolas A, Dumont A, Carita G, et al. Establishment of novel cell lines recapitulating the genetic landscape of uveal melanoma and preclinical validation of mTOR as a therapeutic target. Mol Oncol 2014. https://doi.org/10.1016/j.molonc.2014.06.004.

[12] Carvajal RD, Sosman JA, Quevedo JF, Milhem MM, Joshua AM, Kudchadkar RR, et al. Effect of selumetinib vs chemotherapy on progression-free survival in uveal melanoma: a randomized clinical trial. JAMA, J Am Med Assoc 2014. https://doi.org/10.1001/jama.2014.6096.

[13] Piperno-Neumann S, Kapiteijn E, Larkin JMG, Carvajal RD, Luke JJ, Seifert H, et al. Phase I dose-escalation study of the protein kinase C (PKC) inhibitor AEB071 in patients with metastatic uveal melanoma. J Clin Oncol 2019. https://doi.org/10.1200/jco.2014.32.15_suppl.9030.

[14] Yang J, Manson DK, Marr BP, Carvajal RD. Treatment of uveal melanoma: where are we now? Ther Adv Med Oncol 2018. https://doi.org/10.1177/1758834018757175.

[15] Amirouchene-Angelozzi N, Frisch-Dit-Leitz E, Carita G, Dahmani A, Raymondie C, Liot G, et al. The mTOR inhibitor Everolimus synergizes with the PI3K inhibitor GDC0941 to enhance anti-tumor efficacy in uveal melanoma. Oncotarget 2016. https://doi.org/10.18632/oncotarget.8054.

[16] Carita G, Frisch-Dit-Leitz E, Dahmani A, Raymondie C, Cassoux N, Piperno-Neumann S, et al. Dual inhibition of protein kinase C and p53-MDM2 or PKC and mTORC1 are novel efficient therapeutic approaches for uveal melanoma. Eur J Cancer 2016. https://doi.org/10.1016/s0959-8049(16)32672-7.

[17] Chen X, Wu Q, Tan L, Porter D, Jager MJ, Emery C, et al. Combined PKC and MEK inhibition in uveal melanoma with GNAQ and GNA11 mutations. Oncogene 2014. https://doi.org/10.1038/onc.2013.418.

[18] Khalili JS, Yu X, Wang J, Hayes BC, Davies MA, Lizee G, et al. Combination small molecule MEK and PI3K inhibition enhances uveal melanoma cell death in a mutant GNAQ- and GNA11-dependent manner. Clin Cancer Res 2012. https://doi.org/10.1158/1078-0432.CCR-11-3227.

[19] Musi E, Ambrosini G, de Stanchina E, Schwartz GK. The phosphoinositide 3-kinase α selective inhibitor BYL719 enhances the effect of the protein kinase C inhibitor AEB071 in GNAQ/GNA11-Mutant uveal melanoma cells. Mol Cancer Ther 2014. https://doi.org/10.1158/1535-7163.mct-13-0550.

[20] Heijkants R, Willekens K, Schoonderwoerd M, Teunisse A, Nieveen M, Radaelli E, et al. Combined inhibition of CDK and HDAC as a promising therapeutic strategy for both cutaneous and uveal metastatic melanoma. Oncotarget 2018. https://doi.org/10.18632/oncotarget.23485.

[21] Heijkants RC, Nieveen M, Hart KCT, Teunisse AFAS, Jochemsen AG. Targeting MDMX and PKCδ to improve current

uveal melanoma therapeutic strategies. Oncogenesis 2018. https://doi.org/10.1038/s41389-018-0041-y.

[22] Chen Q, Song S, Wei S, Liu B, Honjo S, Scott A, et al. ABT-263 induces apoptosis and synergizes with chemotherapy by targeting stemness pathways in esophageal cancer. Oncotarget 2015. https://doi.org/10.18632/oncotarget.4540.

[23] Chen J, Jin S, Abraham V, Huang X, Liu B, Mitten MJ, et al. The Bcl-2/Bcl-XL/Bcl-w inhibitor, navitoclax, enhances the activity of chemotherapeutic agents in vitro and in vivo. Mol Cancer Ther 2011. https://doi.org/10.1158/1535-7163.mct-11-0415.

[24] Némati F, De Montrion C, Lang G, Kraus-Berthier L, Carita G, Sastre-Garau X, et al. Targeting Bcl-2/Bcl-X L induces antitumor activity in uveal melanoma patient-derived xenografts. PLoS One 2014. https://doi.org/10.1371/journal.pone.0080836.

[25] Airiau K, Prouzet-Mauléon V, Rousseau B, Pigneux A, Jeanneteau M, Giraudon M, et al. Synergistic cooperation between ABT-263 and MEK1/2 inhibitor: effect on apoptosis and proliferation of acute myeloid leukemia cells. Oncotarget 2016. https://doi.org/10.18632/oncotarget.6417.

[26] Chapeau EA, Gembarska A, Durand EY, Mandon E, Estadieu C, Romanet V, et al. Resistance mechanisms to TP53-MDM2 inhibition identified by in vivo piggyBac transposon mutagenesis screen in an Arf −/− mouse model. Proc Natl Acad Sci 2017. https://doi.org/10.1073/pnas.1620262114.

[27] Duan Z, Chinn D, Tu MJ, Zhang QY, Huynh J, Chen J, et al. Novel synergistic combination of mitotic arrest and promotion of apoptosis for treatment of pancreatic adenocarcinoma. Transl Oncol 2019. https://doi.org/10.1016/j.tranon.2019.01.009.

[28] Coupland SE, Bechrakis N, Schüler A, Anagnostopoulos I, Hummel M, Bornfeld N, et al. Expression patterns of cyclin D1 and related proteins regulating G1-S phase transition in uveal melanoma and retinoblastoma. Br J Ophthalmol 1998. https://doi.org/10.1136/bjo.82.8.961.

[29] Brantley MA, Harbour JW. Deregulation of the Rb and p53 pathways in uveal melanoma. Am J Pathol 2000. https://doi.org/10.1016/s0002-9440(10)64817-1.

[30] Gao H, Korn JM, Ferretti S, Monahan JE, Wang Y, Singh M, et al. High-throughput screening using patient-derived tumor xenografts to predict clinical trial drug response. Nat Med 2015. https://doi.org/10.1038/nm.3954.